Polskie Towarzystwo Materiałów Kompozytowych
Polish Society of Composite Materials

Kompozyty 11: 3 (2011) 230-234

KOMPOZYTY
COMPOSITES

Michał Barcikowski[1]*, Bartosz Semczyszyn[2]

[1] West Pomeranian University of Technology, Polymer Institute, Division of Polymer Materials Technology, ul. Pułaskiego 10, 70-322 Szczecin, Poland
[2] West Pomeranian University of Technology, Polymer Institute, Formerly: Division of Polymer Materials Technology, ul. Pułaskiego 10, 70-322 Szczecin, Poland
Currently: ERMA Sp. z o.o., ul. Światowida 6, 71-726 Szczecin, Poland
** Corresponding author. E-mail: Michal.Barcikowski@zut.edu.pl*

Otrzymano (Received) 01.02.2011

IMPACT DAMAGE IN POLYESTER-MATRIX GLASS FIBRE-REINFORCED COMPOSITES. PART I. IMPACT DAMAGE EXTENT

Fibre-reinforced composites are susceptible to damage resulting from impacts. This damage may lead to a reduction of composite strength and load-bearing abilities, both in static loading as well as during subsequent impact events. Composites with improved tolerance to ballistic impact using inexpensive, common materials i.e. E-glass fibre and unsaturated polyester resin, have been manufactured by means of modern, yet popular moulding technology. Composite materials were reinforced with an E-type glass fibre in the form of a continuous filament mat and woven roving. The fibre content in the composites was varied to evaluate the effect of the reinforcement fraction on impact tolerance. The composites were manufactured using the Resin Transfer Moulding (RTM) method. The extent of damage in glass fibre/polyester composites after non-penetrating ballistic impact has been evaluated. Samples of the manufactured laminates were subjected to impact using a compressed-air gun test assembly. The impactor was a free-flying 3-gram hardened steel sphere, and the impact velocities were up to 125 m/s. After the impact and damage evaluation, the samples were photographed in transmitted light, and the obtained images were digitally processed by software to measure the area of delamination. It was found that the damaged area is directly proportional to the impact energy. Moreover, reinforcement in the form of a continuous-filament mat compares favourably to loose woven roving; such reinforced composites have a much smaller area of delamination after impact of a given energy. The impacted samples were sectioned and imaged microscopically in low magnification. The damage in continuous-filament mat-reinforced composites is visibly less severe than in composites with fabric reinforcement.

Keywords: polymer composites, laminates, unsaturated polyester resin, glass fibre, ballistic impact, damage

USZKODZENIA UDAROWE WE WZMOCNIONYCH WŁÓKNEM SZKLANYM KOMPOZYTACH O MATRYCY POLIESTROWEJ. CZĘŚĆ I. ROZLEGŁOŚĆ USZKODZEŃ UDAROWYCH

Kompozyty wzmocnione włóknami są podatne na uszkodzenia powstałe w wyniku udarów. Uszkodzenia te mogą prowadzić do obniżenia wytrzymałości kompozytów oraz ich zdolności do przenoszenia obciążeń, zarówno przy obciążeniach statycznych, jak i podczas kolejnych zdarzeń udarowych. W pracy podjęta została próba wytworzenia kompozytów o podwyższonej odporności na udar balistyczny z użyciem niedrogich, powszechnie stosowanych materiałów, takich jak włókno szklane typu E i nienasycona żywica poliestrowa, za pomocą nowoczesnej, a jednocześnie popularnej na świecie metody formowania. Wykorzystano kompozyty wzmocnione włóknem szklanym typu E w postaci maty z włókien ciągłych i tkaniny rovingowej. Zawartość włókien w kompozycie była zmieniana w celu zbadania wpływu udziału wzmocnienia na odporność udarową kompozytu. Materiały zostały wytworzone z użyciem metody RTM (*Resin Transfer Moulding*). Przeprowadzono ewaluację rozległości uszkodzeń kompozytów poliestrowo-szklanych po niepenetrującym udarze balistycznym. Próbki wytworzonych laminatów zostały poddane udarowi z użyciem urządzenia udarowego napędzanego sprężonym powietrzem. Impaktorem była swobodna, 3-gramowa kula z utwardzonej stali, a prędkości udarów sięgały 125 m/s. Po udarze oszacowana została rozległość uszkodzeń. W tym celu próbki zostały sfotografowane w świetle przechodzącym i poddane cyfrowej analizie obrazu, aby zmierzyć powierzchnię delaminacji. Pole uszkodzeń okazało się być wprost proporcjonalne do energii udaru. Co jest istotne, materiały wzmocnione matą z włókien ciągłych wypadły korzystnie w porównaniu z tymi wzmocnionymi tkaniną rovingową, tj. cechowały się wyraźnie mniejszym polem uszkodzeń po udarze o danej energii. Próbki po badaniu udarowym zostały przecięte i poddane oględzinom mikroskopowym pod niewielkim powiększeniem. Kompozyty wzmocnione matą z włókien ciągłych odniosły wyraźnie mniej poważne uszkodzenia.

Słowa kluczowe: kompozyty polimerowe, laminaty, nienasycona żywica poliestrowa, włókno szklane, udar balistyczny, uszkodzenia

INTRODUCTION

Fibre-reinforced plastics (FRP) are increasingly common as construction materials that are subjected to a wide range of loading conditions. Among them, the most crucial condition is impact loading [1]. Impact loads may be caused by vehicle collisions, falling objects (common occurrences are dropped tools), hail,

gravel striking vehicles, birds striking aircraft or wind turbine blades etc. The issue of composites resistance to impact loads is a complicated one. Multiple phases and interfaces allow relatively easy dissipation of impact energy, while at the same time lead to irreversible damage. It must be emphasized that energy absorption and damage resistance are to some extent conflicting - the main mode of energy absorption is the damage itself [2].

There are several modes of energy absorption and damage mechanisms in laminated composites. Most frequently cited are the kinetic energy of the displaced part of the target object, fibre tension, fibre destruction through tensile failure or shearing, delamination, matrix cracking as well as friction between the impactor and target material [2-7]. The most important are target kinetic energy and fibre failure [3-6], while delamination and matrix cracking are the primary cause of post-impact strength reduction [2, 5, 7-10]. Since matrix cracking and delamination always occur together - in fact, the former initiates the latter - no attempt to discern between the two damage types is feasible [5].

Impact events may be classified depending on various characteristics, one of the most widely used being the speed of the impact. The materials behave differently when impacted with different velocity especially viscoelastic materials such as plastics. Therefore, impacts may be classified as low-velocity impacts (velocity < 10 m/s) also known as quasi-static (due to stress placement essentially identical to that in static loading), intermediate-velocity impacts (10÷100 m/s), high-velocity impacts (100÷1000 m/s) and hypervelocity impacts (> 1 km/s) [3, 11, 12]. Considering intermediate- and high-velocity impacts, contrary to quasi-static impacts, during the impact event the stress is still propagating through the material in the form of elastic waves, both longitudinal and transversal. The time of the impactor-target contact is too short for these waves to propagate to the edges of the material and back. The damage is thus confined to an area significantly smaller than the entire target object [3, 11, 12]. Intermediate- and high-velocity impacts are typical for objects falling from a significant height (hail for example), gravel striking high-speed cars, runway debris and bird striking aircraft as well as for gunfire or shrapnel fragments. The latter two are by no means insignificant even in civilian applications.

It is important to evaluate the extent of damage in FRP after the impact event. Impact damage in laminates usually consists of the impactor footprint (or hole in the case of complete perforation) and surrounding field of delamination (together with co-occurring matrix cracking). The extent of delamination (and assumed matrix cracking) damage is usually much larger than the impact footprint itself. The area of delamination is supposed to be proportional to the impact energy for non-penetrating impacts [8, 9, 13]. The delaminated area is usually well visible; thus, the easiest way to evaluate the extent of damage is optical - either by the researcher's eye or using instrumentation and digital image processing. Images for the analysis are obtained through either photography or scanning [2, 10, 14-19]. Other, non-optical methods are sometimes used - ultrasonic C-scan [8, 9, 20-22] or X-ray tomography [13, 21].

MATERIALS

Multi-ply composites (laminates) made of unsaturated polyester (UP) resin and E-type glass fibre in various forms were used. The laminates were produced using a resin transfer moulding (RTM) method in a stiff double mould. In this method, a resin, driven by overpressure, infuses the closed mould cavity and permeates the reinforcement placed there. The laminates were manufactured in the form of flat, square plates with a thickness of 4 mm.

The common element for all the composites in this study was the matrix of UP resin Polimal 109-32K, produced by Z. Ch. "Organika-Sarzyna" S.A. (Poland). It is a general-purpose, construction-grade, rigid, ortophtalic resin. The resin was cured via free-radical copolymerisation initiated by a 1.5% addition of methylethylketone peroxide (MEKP) solution in dimethyl phthalate produced under the name Metox-50 by Oxytop Ltd. (Poland). Curing was promoted by an admixture of 0.6 ml of 10% cobalt accelerator (cobalt (II) hexanoate solution in organic solvent) per 1 kg of resin.

The laminates were reinforced using E-type glass fibre in the form of a varying number of plies of mat or fabric. Two types of reinforcement were used:

- Vetrotex Unifilo-series U750 450-138 continuous-filament mat (CFM) with weight of 450 g/m^2, bound with thermoplastic polyesters, with silane sizing,
- Vetrotex RC430 woven roving (WR) with twill weave (4x1) and weight of 430 g/m^2, with finish for polyesters.

The weight of both reinforcements is similar enough to allow direct substitution of one of them by the other on a ply-for-ply basis without significantly influencing other parameters.

Using these reinforcements, three different composites were produced:

1. 6CFM45 - six plies of 450 g/m^2 CFM combining to total area weight of 2700 g/m^2 and reinforcement weight fraction 44% (volume fraction 27%, porosity 2.5%).
2. 6WR43 - six plies of 430 g/m^2 WR combining to total area weight of 2580 g/m^2 and reinforcement weight fraction 42% (volume fraction 26%, porosity 3.2%), in $[0°/90°]_3$ lay up
3. 10WR43 - ten plies of 430 g/m^2 WR combining to total area weight of 4300 g/m^2 and reinforcement weight fraction 61% (volume fraction 43%, porosity 3.5%), in $[0°/90°]_5$ lay up.

The low reinforcement fraction for the CFM-reinforced composite is caused by the low compressibil-

ity of mats compared to woven fabrics [23]. Woven roving allows a higher level of compression. No differentiation of ply direction in the CFM-reinforced composite was deemed necessary.

TABLE 1. **Static tensile properties of composites used in study according to ISO 527:4-1997**
TABELA 1. **Statyczne właściwości przy rozciąganiu kompozytów użytych do badań, wg ISO 527:4-1997**

Material	Strain at peak stress [%]	Standard deviation [%]	Peak stress [MPa]	Standard deviation [MPa]	Young's modulus [MPa]	Standard deviation [MPa]
6WR43	2.393	0.166	129.3	4.8	8013	355
10WR43	3.113	0.309	179.3	12.1	9611	726

The reinforcement weight and volume ratios were obtained via calcination. The porosity was determined through density measurement. The static tensile properties were obtained according to ISO 527:4-1997.

The laminates were cut into square plate samples 100x100 mm using a diamond saw.

TESTING

The composites in this study were subjected to impact using a compressed-air gun test assembly (Fig. 1).

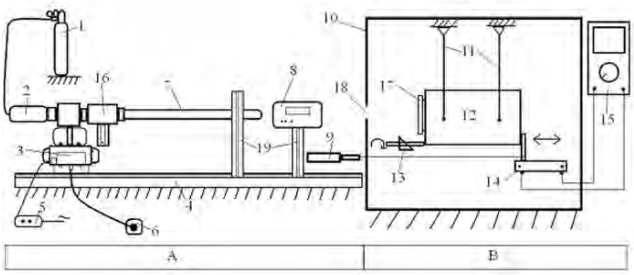

Fig. 1. Compressed-air gun test assembly schematics: A - propelling part, B - ballistic pendulum with shield casing, 1 - compressed air cylinder, 2 - intermediate compressed air reservoir, 3 - electropneumatic valve, 4 - cradle, 5 - triggering switch, 6 - connection to compressed air grid, 7 - barrel, 8 - ballistic chronograph, 9 - potentiometer-zeroing dynamometer, 10 - ballistic pendulum shield, 11 - ballistic pendulum suspension, 12 - ballistic pendulum, 13 - pendulum zeroing device, 14 - potentiometer, 15 - measuring device, 16 - gun breech, 17 - sample frame, 18 - shield opening, 19 - barrel and chronograph mount.

Rys. 1. Schemat stanowiska do badań udarowych: A - Część napędowa, B - Wahadło balistyczne z osłoną, 1 - butla ze sprężonym powietrzem, 2 - zbiornik pośredni sprężonego powietrza, 3 - zawór elektropneumatyczny, 4 - szyna montażowa, 5 - przycisk wyzwalania, 6 - podłączenie do sieci sprężonego powietrza, 7 - prowadnica impaktora, 8 - chronograf balistyczny, 9 - dynamometr do zerowania potencjometru, 10 - osłona wahadła balistycznego, 11 - zawieszenie wahadła balistycznego, 12 - wahadło balistyczne, 13 - przyrząd do zerowania wahadła, 14 - potencjometr, 15 - miernik, 16 - część zamkowa, 17 - ramka na próbki, 18 - otwór w osłonie, 19 - podpory prowadnicy i chronografu

The gas gun propels impactors in the form of steel balls, 9.0 mm in diameter and 3.0 g in weight, by means of compressed air stored in a tank. The impactor muzzle velocity is measured by an attached ballistic chronograph. The difference between the muzzle and incident velocity is deemed negligible due to the short distance between the barrel muzzle and the sample. The impactor velocity was varied by varying the compressed air pressure. The tests in this study encompassed velocities in the range of 90÷130 m/s, resulting in impact energies in the range of 12÷25 J.

Samples with the aforementioned dimensions - square plates 100x100x4 mm - were secured to the front of a ballistic pendulum, supported in four corners.

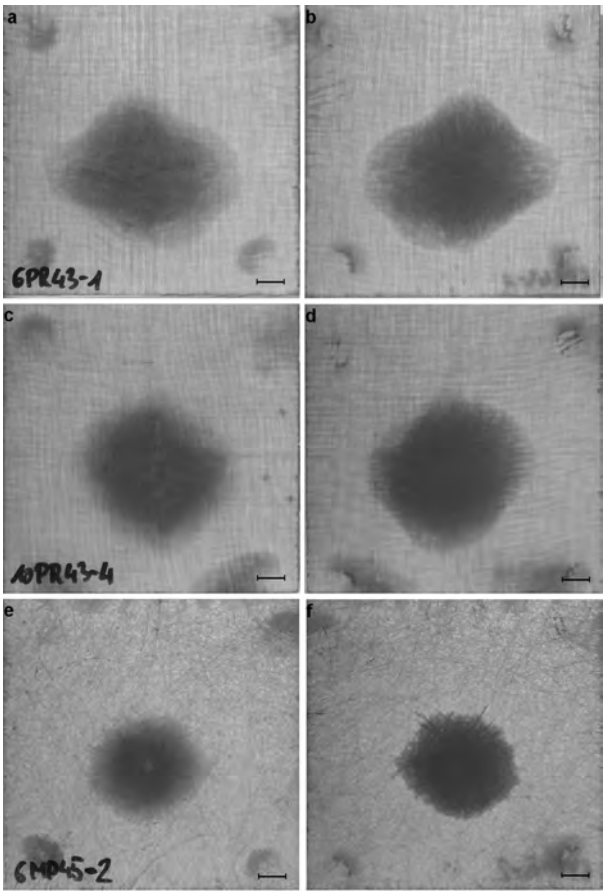

Fig. 2. Transmitted light images of selected samples after impact (damage visible): a) front (impacted) side of 6WR43 sample, b) back side of 6WR43 sample, c) front (impacted) side of 10WR43 sample, d) back side of 10WR43 sample, e) front (impacted) side of 6CFM45 sample, f) back side of 6CFM45 sample

Rys. 2. Obrazy w świetle przechodzącym wybranych próbek po udarze (widoczne uszkodzenia): a) strona czołowa kompozytu 6WR43, b) strona tylna kompozytu 6WR43, c) strona czołowa kompozytu 10WR43, d) strona tylna kompozytu 10WR43, e) strona czołowa kompozytu 6CFM45, f) strona tylna kompozytu 6CFM45

The extent of delamination (co-occurring with matrix cracking) was evaluated by means of digital image analysis - the samples were photographed in transmitted light using a digital camera. The obtained images (Fig. 2) were processed using Scion Image software to measure the contrasting delaminated area.

Afterwards, the samples were either sectioned and imaged in low magnification with a Bresser HDM

1.3 MP microscope or used in residual strength tests (see Part II of the paper).

RESULTS AND DISCUSSION

In Figure 3, the close-up views of the impacted and un-impacted samples are shown. The damage is readily visible, mainly in the form of matrix cracking. The composites reinforced with woven roving (6WR43 and 10WR43) also show some amount of fibre fracture and a substantial increase in thickness due to delamination. In the composite reinforced with continuous--filament mat (6CFM45) delamination is also present, though not with the same effect on thickness. It may be presumed that the severity of damage is also lower. Figure 4 presents the periphery of the area damaged during impact. It is clear that the damage extends further from the impact point at greater depths. That is congruent with the quasi-cone shape of damaged volume known from literature.

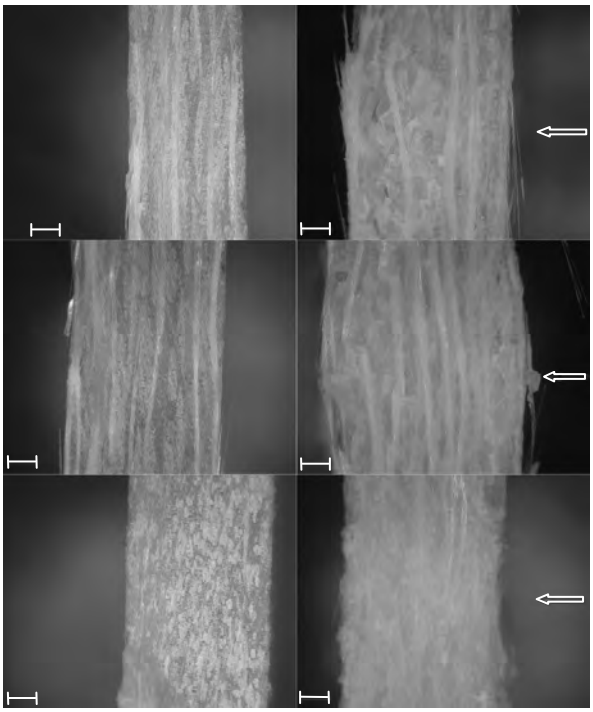

Fig. 3. Low-magnification microscopic views of samples. Left column - undamaged samples, right column - centre of damaged area after 22 J impact; top row - 6WR43, middle row - 10WR43; bottom row - 6CFM45. Arrows show direction and centre of impact. Scale bar is 1 mm

Rys. 3. Mikrografie próbek przy niewielkim powiększeniu. Lewa kolumna - próbki nieuszkodzone, prawa kolumna - centrum obszaru uszkodzonego w wyniku udaru o energii 22 J; górny rząd - 6WR43, środkowy rząd - 10WR43, dolny rząd - 6CFM45. Strzałki wskazują kierunek i centrum uderzenia. Marker oznacza 1 mm

Figure 5 presents the area of delamination vs. impact energy graph. The delaminated field area depends virtually linearly (correlation coefficient of 0.987÷0.996) on the impact energy; it is to be expected based on the accounts in literature [8, 9, 13]. The extrapolated y-intercept seems to be zero as expected, because zero-energy impacts (i.e. no impact at all) result in no damage. The equations for the lines of regression ($y = Ax + B$) for the three materials, from which the values of slope (A) and y-intercept (B) may be made out, as well as the calculated coefficient of determination (R^2), are presented on the graph.

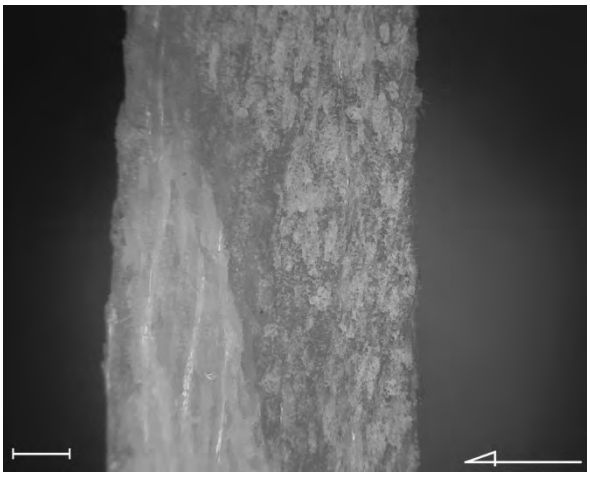

Fig. 4. Low magnification of microscopic view of periphery of damage area after 22 J impact in 6CFM45 sample. Arrow shows direction of impact (centre of impact lies beyond image limits). Scale bar is 1 mm

Rys. 4. Mikrografia przy niewielkim powiększeniu peryferiów obszaru uszkodzonego w wyniku udaru o energii 22 J próbki kompozytu 6CFM45. Strzałka wskazuje kierunek uderzenia (centrum uderzenia leży poza granicami obrazu). Marker oznacza 1 mm

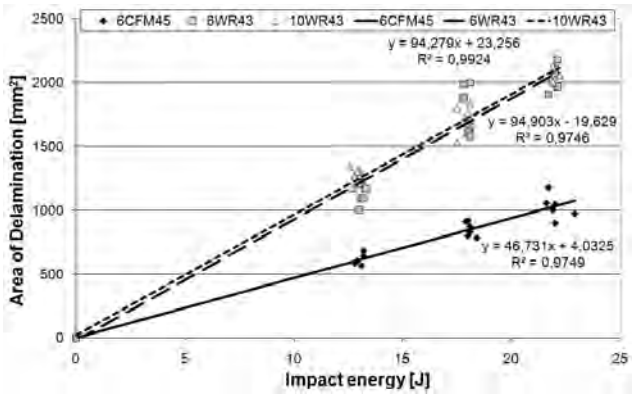

Fig. 5. Delamination vs. impact energy graph

Rys. 5. Wykres zależności powierzchni delaminacji od energii udaru

Comparing two composites with a differing content of woven roving reinforcement, there is almost no difference between the two regression lines. Surprisingly, there seem to be no delaminated area dependence on the reinforcement content. In contrast, the CFM-reinforced composite undergoes much less delamination when subjected to a comparable impact - the slope for CFM is a bit below 50% of the WR slope (46.7 mm^2/J compared to 94.2÷94.9 mm^2/J). This posits that the continuous filament mat as reinforcement leads to higher impact tolerance than woven roving, undoubtedly due to structural differences.

CONCLUSION

In the course of this study, it was shown that the area delaminated as a result of an impact is directly proportional to the impact energy and no vertical offset is expected nor found.

Continuous-filament mats are superior to loose-structure woven rovings - the damaged area after the impact with a given energy is lower in CFM-reinforced composites than in WR-reinforced ones. The damage as seen in the cross-section is also less severe in CFM-reinforced composites. This is worth noting and needs further investigation.

Acknowledgements

This work was partially financed by the Ministry of Science and Higher Education of the Republic of Poland in project 15-78-9504/15-00-00.

The authors would like to thank Mr. Marek Żwir for his contribution to this work.

REFERENCES

[1] Avila A.F., Soares M.I., Neto A.S., A study on nanostructured laminated plates behavior under low-velocity impact loading, International Journal of Impact Engineering 2007, 34, 28-41.

[2] Schrauwen B., Peijs T., Influence of matrix ductility and fibre architecture on the repeated impact response of glass-fibre-reinforced laminated composites, Applied Composite Materials 2002, 9, 331-352.

[3] Naik N.K., Shrirao P., Composite structures under ballistic impact, Composite Structures 2002, 66, 579-590.

[4] Hetherington J.G., Energy and momentum changes during ballistic perforation, International Journal of Impact Engineering 1996, 18, 319-337.

[5] Kang T.J., Kim C., Energy-absorption mechanisms in Kevlar multiaxial warp-knit fabric composites under impact loading, Composite Science and Technology 2000, 60, 773--784.

[6] Morye S.S., Hine P.J., Ducket R.A., Carr D.J., Ward I.M., Modelling of the energy absorption by polymer composites upon ballistic impact, Composite Science and Technology 2000, 60, 2631-2642.

[7] Naik N.K., Shrirao P., Reddy B.C.K., Ballistic impact behaviour of woven fabric composites: Formulation, International Journal of Impact Engineering 2006, 32, 1521-1552.

[8] Reis L., de Freitas M., Damage growth analysis of low velocity impacted composite panels, Composite Structures 1997, 38, 509-515.

[9] Hosur M.V., Karim M.R., Jeelani S., Experimental investigation on the response of stitched/unstitched woven S2-glass/SC15 epoxy composites under single and repeated low velocity impact loading, Composite Structures 2003, 61, 89--102.

[10] da Silva Jr J.E.L., Paciornik S., d'Almeida J.R.M., Determination of the post-ballistic impact mechanical behaviour of a ±45° glass-fabric composite, Polymer Testing 2004, 23, 599-604.

[11] Cheeseman B.A., Bogetti T.A., Ballistic impact into fabric and compliant composite materials, Composite Structures 2003, 61, 161-173.

[12] Olsson R., Mass criterion for wave controlled impact response of composite plates, Composites Part A 2000, 31, 879-887.

[13] DeLuca E., Prifti J., Betheney W., Chou S.C., Ballistic impact damage of S 2-glass-reinforced plastic structural armour, Composite Science and Technology 1997, 58, 1453-1461.

[14] Zhang Z.Y., Richardson M.O.W., Low velocity impact induced damage evaluation and its effect on the residual flexural properties of pultruded GRP composites, Composite Structures 2007, 81, 195-201.

[15] Shyr T.-W., Pan Y.-H., Impact resistance and damage characteristics of composite laminates, Composite Structures 2003, 62, 193-203.

[16] Walker L., Sohn M.-S., Hu X.-Zh., Improving impact resistance of carbon-fibre composites through interlaminar reinforcement, Composites Part A 2002, 33, 893-902.

[17] Park R., Jang J., Effect of laminate thickness on impact behavior of aramid fiber/vinylester composites, Polymer Testing 2003, 22, 939-946.

[18] Da Silva Jr J.E.L., Paciornik S., d'Almeida J.R.M., Evaluation of the effect of the ballistic damaged area on the residual impact strength and tensile stiffness of glass-fabric composite materials, Composite Structures 2004, 64, 123-127.

[19] Barcikowski M., Remaining strength in glass-polyester laminated composites subjected to ballistic impact, Kompozyty (Composites) 2009, 9, 271-275.

[20] Hosur M.V., Vaidya U.K., Ulven C., Jeelani S., Performance of stitched/unstitched woven carbon/epoxy composites under high velocity impact loading, Composite Structures 2004, 64, 455-466.

[21] Imielinska K., Castaings M., Wojtyra R., Haras J., Le Clezio E., Hosten B., Air-coupled ultrasonic C-scan technique in impact response testing of carbon fibre and hybrid: glass, carbon and Kevlar/epoxy composites, Journal of Materials Processing Technology 2004, 157-158, 513-522.

[22] Tarim M., Findik F., Uzun H., Ballistic impact performance of composite structures, Composite Structures 2002, 56, 13--20.

[23] Somashekar A.A., Bickerton S., Bhattacharyya D., Exploring the non-elastic compression deformation of dry glass fibre reinforcements, Composite Science and Technology 2007, 67, 183-200.

